

Original Article

Design and Analysis of Compact Giraffe-Shaped Patch Antenna for UWB Applications: A FDTD and Hybrid PSO Algorithm Approach

Girish Bhide¹, Brijesh Iyer², Anil Nandgaonkar³, Sanjay Nalbalwar⁴ and Abhay Wagh⁵

¹Research Scholar, Dr. Babasaheb Ambedkar Technological University, Lonere, Raigad 402103, India

²Assistant Professor, Dr. Babasaheb Ambedkar Technological University, Lonere, Raigad 402103, India

^{3,4}Professor, Dr. Babasaheb Ambedkar Technological University, Lonere, Raigad 402103, India

⁵ Director, Directorate of Technical Education, Maharashtra, MUMBAI, 40001, India

ggb_rtn@yahoo.co.in, brijeshiyer@dbatu.ac.in, abnandgaonkar@dbatu.ac.in

Abstract — This paper reports a compact ultra-wideband (UWB) Giraffe-shaped patch antenna designed using hybrid particle swarm optimization (HPSO) algorithm. The shape of the rectangular microstrip antenna is divided into multiple small squares called pixels. These pixels are assigned binary values 1 or 0 based on decision criteria into the algorithm, known as a fitness function. The optimization algorithm implemented in the HFSS platform removes the pixels with value 0 and achieves ultra-wideband performance for the antenna within three iterations. The FDTD analysis using the convolutional perfectly matched layer (CPML) technique is used to validate the HFSS simulation results. The antenna is fabricated on an FR4 substrate with a permittivity of 4.4. The overall size of the antenna is 14 mm x 25.8 mm x 1.6 mm. The measured gain of the antenna ranges from 2.95 dBi to 4.45 dBi over the operating frequency range 3.2 GHz to 9.8 GHz. The measurement results show the best agreement with the HFSS simulation and FDTD analysis results.

Keywords — FDTD analysis, Giraffe-shaped patch antenna, Hybrid particle swarm optimization algorithm, MATLAB coding, Ultra-wideband antennas.

I. INTRODUCTION

Ultra-wideband (UWB) antennas have a variety of applications, including microwave imaging, handheld devices for personal area network (PAN), positioning, RFIDs, through the wall imaging, ground-penetrating radar (GPR), breast tumour detection, etc. The Federal Communications Commission (FCC) approved the 3.1 GHz to 10.6 GHz band as UWB spectrum in 2002; since then, particular attention has been received to design the UWB antenna in this range [1]. Several techniques available in the literature for the design of UWB antennas are discussed here.

An antenna with a double Y-shape slot that provides high gain and circular polarization has been reported by J. Wei et al. [2]. A broken heart shape antenna exhibiting ultra-wideband performance is discussed in Rahman et al. [3]. A Vivaldi antenna using a stepped connection structure has been reported in Wu et al. [4]. An antenna

having an elliptic shape with a central circular slot is discussed by Azenui and Yang [5]. The design of the antenna using three identical pairs of printed half-wave dipoles and its analysis using finite difference time domain (FDTD) is reported by Chengyang Yu et al. [6]. Gong et al. [7] said an antenna uses a compact slot. An antenna using a dual-band fork-shaped monopole is written by Mishra et al. [8]. A modified rectangular plus-shaped antenna is reported in Deshmukh and Mohadikar [9]. An antenna with a stepped triangular shape using the PSO algorithm is written in Trimukhe and Hogade [10]. All these antennas are centred around a compact size design. Recently the use of PSO has gained popularity to design compact UWB antennas. A hexagonal patch structure designed using PSO is reported in Bhattacharya et al. [11]. An improved PSO with neighbourhood-dispatch (NR-PSO) techniques is explained in Li et al. [12]. The ground plane's effect on the performance of multiband PIFA antenna using GA and PSO is discussed in Wakrim and Ibnyaich [13]. A MIMO antenna performing over the UWB band is discussed in [14].

This article discusses the work that uses a hybrid PSO algorithm to optimize the antenna for bandwidth enhancement. The primary antenna structure is developed using Ansys HFSS. The simulation results are fed into the hybrid PSO algorithm implemented in PYTHON.

The antenna performance is also validated using the computational electromagnetics method, FDTD [15]-[16]. The antenna's geometry can be created using this resource's MATLAB code "define geometry" [16]. The details of antenna design and geometry are given in section II. Section III discusses the FDTD analysis of the proposed antenna. The results and discussions are presented in section IV, along with the qualitative analysis of the proposed antenna. Finally, section V consists of the conclusions and future scope.

II. ANTENNA DESIGN AND GEOMETRY

The antenna shape design is done with the objective of wideband response. A rectangular shape is modified using the PSO algorithm in association with high-frequency simulation software (HFSS). Thus, the



simulation software HFSS is not used to implement the algorithm. Instead, the PYTHON platform is used. It reduces computational complexity since the simulation and algorithm are executed on different platforms. This combination is labelled as HPSO, explained in the next section.

A. Hybrid PSO Algorithm

The block diagram of HPSO is depicted in fig. 1. The initial rectangular antenna designed as per the specifications is simulated in HFSS. The optimization parameters, logic, and fitness function are decided using these results. Now antenna simulation results are fed to the algorithm implemented in PYTHON. The algorithm searches and removes pixels that do not meet the set criteria. The microstrip grammar rules are then applied to generate the antenna shape [17]. The simulation of an antenna with a modified shape is again done in HFSS. The results extracted are fed to the algorithm iteratively. This process continues unless and until the design criteria are met. This algorithm can produce unique shaped antennas. One can set the criteria to make band notches, dual-band or multiband antennas, for improving antennas' existing bandwidth, which is specific to the design goal [18]-[19].

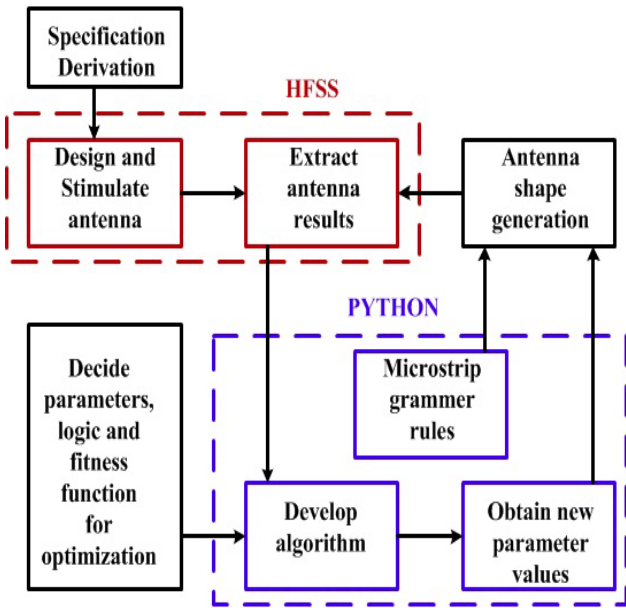


Fig. 1 Hybrid PSO (HPSO) algorithm

In the proposed design, initially, the substrate area was divided into equal squares of array $m \times n$. The values of m and n are decided as per the fine mesh settings used in FDTD analysis. Here m indicates a number of pixels in the

“x” direction, while n indicates a number of pixels in the “y” direction. The substrate size is 14 mm x 25.8 mm x 1.6 mm, which means an area of 361.2 mm². Each square pixel is of size 0.1 mm x 0.1 mm. The calculations for a total number of pixels, m , and n , are shown below in eq.(1- 3).

$$\text{total number of pixels} = \frac{361.2}{0.1 \times 0.1} = 36120 \quad (1)$$

$$m = \frac{14}{0.1} = 140 \quad (2)$$

$$n = \frac{25.8}{0.1} = 258 \quad (3)$$

The selection criterion was applied, then to find out which pixels meet the criterion. All such pixels meeting the criterion were assigned value 1, rest of the pixels were given value 0. At the convergence of the algorithm, this data was fed into antenna simulation software, all the pixels marked with value 0 were eliminated, and simulation was carried out. Once antenna simulation results are generated from simulation software, i.e., HFSS, results are extracted, the algorithm evaluates the fitness function. Keeping the ultra-wideband specifications in mind, the fitness function is given in eq.(4) is used.

$$F(x) = (S_{11_{3.1\text{GHz}}} - S_{11_{\text{acceptable}}}) \cdot u(S_{11_{10.5\text{GHz}}} - S_{11_{\text{acceptable}}}) + \left(\frac{A_3}{A_1} - 1\right) \quad (4)$$

In eq.(4), u is a Heaviside step function having values either 0 or 1. A_3 is the aperture of iteration 3, and A_1 is the aperture of iteration 1. This fitness function depends on the return loss value of the antenna. The acceptable return loss value is set to be -10 dB [20]. Aperture areas are calculated from combined areas of pixels having value 1 as per the S_{11} acceptable criterion. Here A_3 is not the final iteration. One can wait till iteration number 7 and converge the algorithm. In such a case, the numerator in the equation will be A_7 .

In the algorithm, a pixel is treated as a particle. The equations below make the algorithm's basic steps derived from particle swarm optimization. As given in eq (5), we can write the pixel position for i th iteration and m th pixel.

$$p_{i+1}^m = p_i^m + v_{i+1}^m \quad (5)$$

Where v_{i+1}^m Is pixel value change velocity. Generalized pseudo-code followed for optimization is given in Table 1.

Table 1. Pseudocode For PSO Optimization

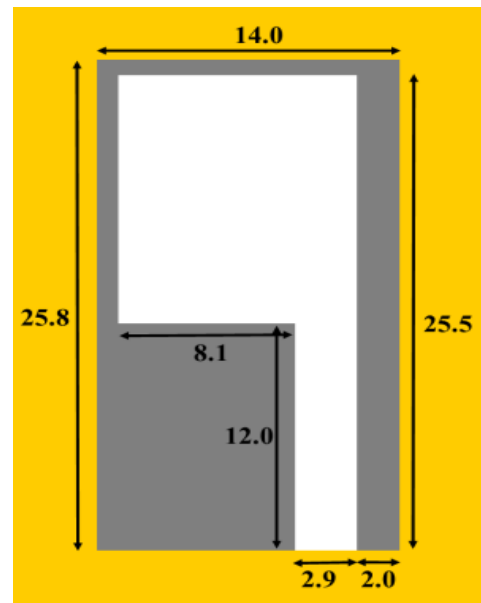
```

For each pixel  $p$ 
  For each limit  $d$ 
    Initialize  $p_i^m$  randomly within dimensions of the antenna.
    Initialize  $v_i^m$  randomly within the distribution of the antenna.
  End
End
Iteration  $i=1$ 
Do
  For each pixel  $p$ 
    Calculate fitness function value,  $fitval$ .
    If  $fitval$  is better than  $p_{best}^m$  in history
      Set current fitness value as  $p_{best}^m$  and set  $b=1$  for pixel  $p$ 
    Else keep  $fitval$  as  $p_{best}^m$  in history and set  $b=0$  for pixel  $p$ 
  End
  Choose pixels having the best  $fitval$ 
  as  $global\ best$ .
  For each pixel  $p$ 
    For each limit  $d$ 
      Calculate velocity for each pixel and apply grammar rules.
      Update particle position
      Generate matrix  $b$ .
    End
  End
Iteration  $i+1$ 
While set iterations reached

```

B. Evolution of the Antenna Shape

The HPSO algorithm is used iteratively to develop the antenna shape for ultra-wideband operation. The rough contours generated are smoothed using grammar rules [17]. In iteration 1, the algorithm has removed the top left side triangular portion of the rectangular patch. In iteration 2, the algorithm removed the strip near the lower part and a small portion at the top right side of the rectangular patch. In iteration 3, the algorithm removed some portions on either side of the strip feed line and some portions near the centre of the patch. The shape obtained in the third iteration is quite similar to the head of the animal "Giraffe", hence included in the title. The original rectangular patch and ground plane are shown in fig. 2 and fig.3, respectively. The ground plane is common for all the iterations. The evolution of the patch (top side) after iteration one is shown in fig.4. Similarly, the patch after iteration two is shown in fig. 5. The patch after iteration 3, which is the final shape looking like a Giraffe head, is shown in fig. 6. The dimensions of the antenna shown in fig. 2 to 6 are in mm.

**Fig. 2 Rectangular Patch**

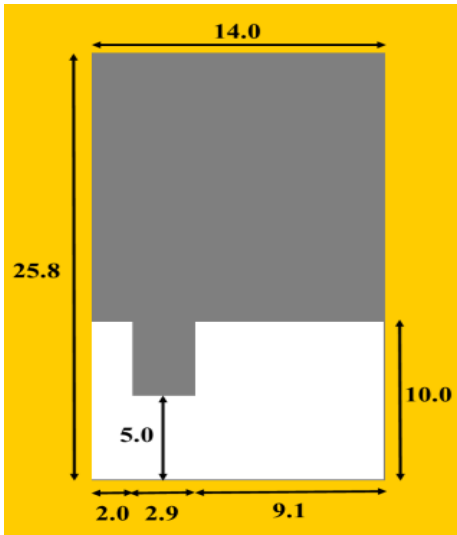


Fig. 3 Ground Plane

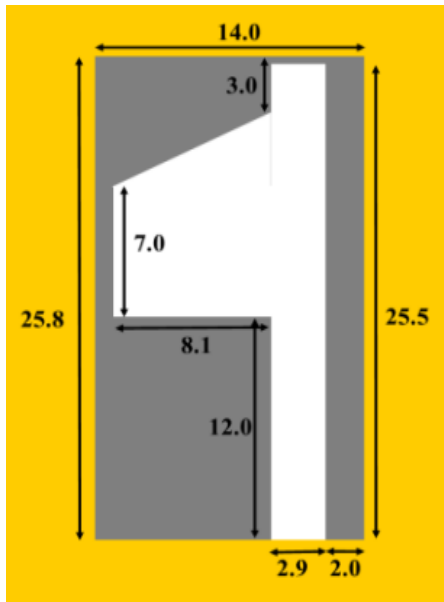


Fig. 4 Iteration 1

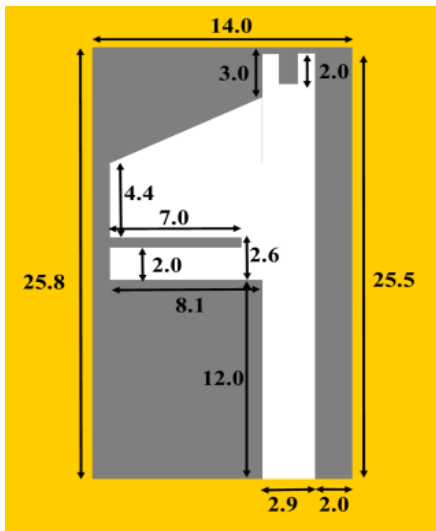


Fig. 5 Iteration 2

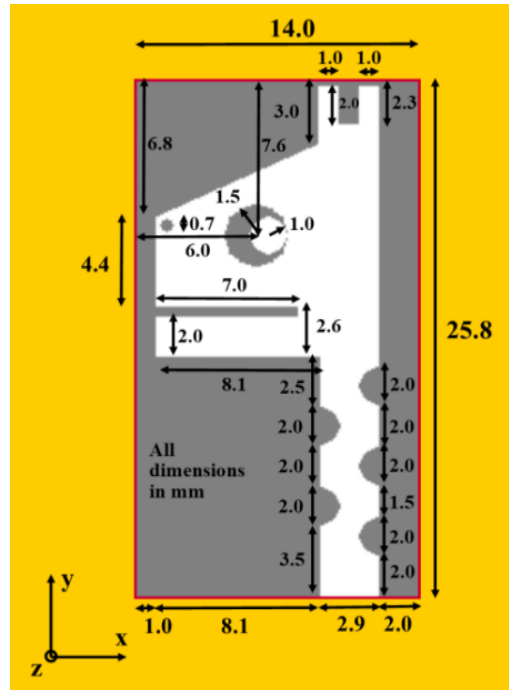


Fig. 6 Iteration 3 - Giraffe Shaped Antenna

C. Simulation Results

The HFSS simulation results of S_{11} were obtained for a rectangular shape, and all three iterations are given in fig. 7. It is observed from the simulation results that S_{11} improved from dual-band to triple band and then to ultra-wideband as the iteration number is increased. The -10 dB bandwidth obtained in final iteration 3 (Giraffe-shaped) is from 2.9 GHz to 10.2 GHz.

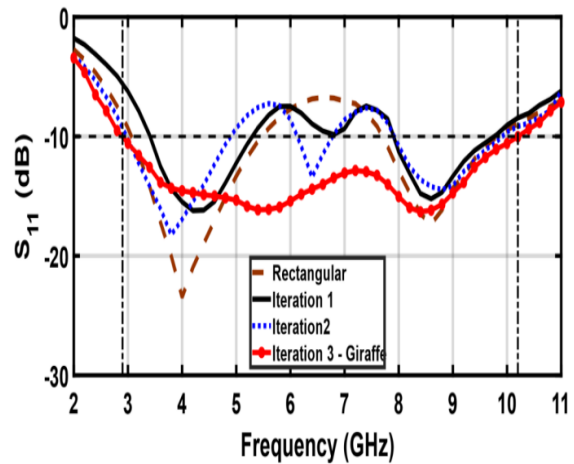


Fig. 7 Simulated S_{11} Results

III. FDTD ANALYSIS

The validation of HFSS simulation results is carried out using one of the most widely used computational electromagnetics methods, FDTD. There are many variants of FDTD based on boundary conditions, such as uniaxial perfectly matched layer FDTD (UPML-FDTD), CPML-FDTD, etc. The reference book used by us titled “The Finite-Difference Time-Domain Method for Electromagnetics with MATLAB Simulations” is based on

CPML-FDTD [16]. The introduction to CPML-FDTD is given here in brief for ready reference.

The electric field intensity, E_x and magnetic field intensity, H_y , are given below in eq.(6, 7), respectively, which express the indexing scheme in the computational domain. The other components follow the same pattern cyclically.

$$E_x(i, j, k) \Rightarrow ((i - 0.5)\Delta_x, (j - 1)\Delta_y, (k - 1)\Delta_z) \quad (6)$$

$$H_y(i, j, k) \Rightarrow ((i - 0.5)\Delta_x, (j - 1)\Delta_y, (k - 0.5)\Delta_z) \quad (7)$$

Maxwell's curl equations are expressed using finite differences as shown in eq. (8).

$$\frac{\partial E_x}{\partial t} = \frac{1}{\epsilon_x} \left(\frac{\partial H_z}{\partial y} - \frac{\partial H_y}{\partial z} - \sigma_x^e E_x - J_{ix} \right) \quad (8)$$

Equation (9) is an expansion of equation 8 using the above indexing scheme.

$$\begin{aligned} & \frac{E_x^{n+1}(i, j, k) - E_x^n(i, j, k)}{\Delta t} \\ &= \frac{1}{\epsilon_x(i, j, k)} \frac{H_z^{n+\frac{1}{2}}(i, j, k) - H_z^{n+\frac{1}{2}}(i, j - 1, k)}{\Delta y} \\ & - \frac{1}{\epsilon_x(i, j, k)} \frac{H_y^{n+\frac{1}{2}}(i, j, k) - H_y^{n+\frac{1}{2}}(i, j, k - 1)}{\Delta z} \\ & - \frac{\sigma_x^e(i, j, k)}{\epsilon_x(i, j, k)} E_x^{n+\frac{1}{2}}(i, j, k) - \frac{1}{\epsilon_x(i, j, k)} J_{ix}^{n+\frac{1}{2}}(i, j, k) \end{aligned} \quad (9)$$

After some manipulations, equation 6 can be expressed with the help of coefficients, as shown in eq. (10).

$$\begin{aligned} E_x^{n+1} &= C_{exe}(i, j, k) \times E_x^n(i, j, k) + C_{exhz}(i, j, k) \\ & \times \left(H_z^{n+\frac{1}{2}}(i, j, k) - H_z^{n+\frac{1}{2}}(i, j - 1, k) \right) \\ & + C_{exhy}(i, j, k) \\ & \times \left(H_y^{n+\frac{1}{2}}(i, j, k) - H_y^{n+\frac{1}{2}}(i, j, k - 1) \right) \\ & + C_{exj}(i, j, k) \times J_{ix}^{n+\frac{1}{2}}(i, j, k) \end{aligned} \quad (10)$$

Where

$$C_{exe}(i, j, k) = \frac{2\epsilon_x(i, j, k) - \Delta t \sigma_x^e(i, j, k)}{2\epsilon_x(i, j, k) + \Delta t \sigma_x^e(i, j, k)}$$

$$C_{exhz}(i, j, k) = \frac{2\Delta t}{(2\epsilon_x(i, j, k) + \Delta t \sigma_x^e(i, j, k))\Delta y}$$

$$C_{exhy}(i, j, k) = -\frac{2\Delta t}{(2\epsilon_x(i, j, k) + \Delta t \sigma_x^e(i, j, k))\Delta z}$$

$$C_{exj}(i, j, k) = -\frac{2\Delta t}{2\epsilon_x(i, j, k) + \Delta t \sigma_x^e(i, j, k)}$$

A. Geometry Implementation in FDTD

The success of FDTD analysis of a microstrip patch antenna mainly depends upon the correct implementation of the antenna's geometry. The FDTD analysis of microstrip patch antenna is done previously but not for an antenna having such a compact size and irregular shape [21]-[25].

The algorithm for this implementation is developed in this work. This implementation is nothing but the correct formation of bricks of the desired material such as dielectric and perfect electric conductors. The antenna shape obtained in the third iteration is implemented in the code routine called "define geometry" using the actual dimensions. The final shape of the proposed antenna is non-regular, containing a triangular edge, rectangular slot and semicircular slots. Therefore, the shape is divided into different contiguous rectangular sections; the algorithm for writing the code for geometry implementation is given in table 2.

Table 2. Algorithm for geometry implementation

Step Number	Action
1)	Sketch the antenna shape on paper.
2)	Mark long contiguous rectangular regions (bricks) in vertical and horizontal directions to cover most of the portion of the antenna.
3)	Note down the coordinates of corners of these bricks as per the xyz frame.
4)	Identify the rectangular portions in which the semicircular slots are to be created.
5)	Do not delete any brick already created. If there is a need of deleting a brick go back to step number 2) and reorganize the bricks since there will be an error at the time of implementation if any brick is deleted.
6)	Obtain the coordinates of corners of small rectangles surrounding the semicircular slots.
7)	Fill the region outside the semicircular slots with small rectangles identified in step number 6).
8)	Use "for loop" for creating triangular and or circular sections using rectangles which was not covered earlier.
9)	The circular shape extending into the slots be developed at the end.
10)	Compare the developed shape with the desired one for accuracy.

The triangular, semicircular, and circular portions within the geometry of the antenna can be achieved using novel image algorithms developed by Bhide et al. [26]. The

complete code for the generation of antenna geometry developed by us using the above algorithm given in Table 2 is of around 1000 lines.

The implementation of the geometry using the MATLAB code is shown in fig. 8, which exactly matches with the final Giraffe shape obtained using the HPSO. The long contiguous regions (bricks) mentioned in step number 2) of the algorithm in Table 2 are clearly visible. The shaded portions also consist of bricks but of very small sizes created using steps numbers 6) to 8) of the algorithm. There are a total of 173 bricks used for the implementation of the geometry. Out of this, one brick was used for the substrate, 3 for the ground plane, 21 big to medium size bricks (visible in fig. 8 with pink colour), and the remaining 148 small size bricks to make up the various semicircular, circular, and triangular shapes on the top side (patch). Once the geometry is developed, the main routine called “fdtd solve” from the resource is run to obtain the antenna's return loss and radiation pattern.

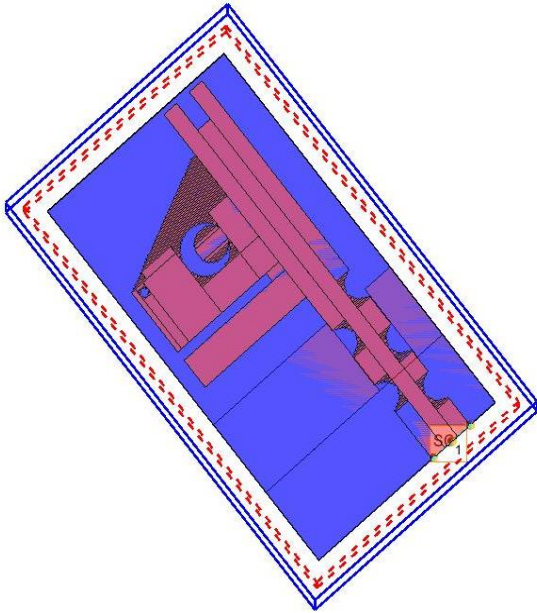


Fig. 8 The geometry of the antenna developed using MATLAB code

B. FDTD Setup

The substrate size is 14 mm x 25.8 mm x 1.6 mm. Further, the shape of the antenna contains many circles and semicircles, wherein the radius of the smallest circle is 0.35 mm. It was therefore decided to use a fine mesh for discretization. The values selected are $dx = 0.1$ mm, $dy = 0.1$ mm, and $dz = 0.4$ mm. The formula for calculating the number of cells in the “x” direction called “nx” is given by eq. (11). The actual calculations for “nx”, “ny”, and “nz” is shown in eq. (12 – 14) respectively.

$$nx = \frac{\text{length in } x \text{ direction}}{dx} + 2(\text{CPML buffer cells} + \text{Air buffer cells}) \quad (11)$$

$$nx = \frac{14 \text{ mm}}{0.1 \text{ mm}} + 2(8 + 10) = 176 \quad (12)$$

$$ny = \frac{25.8 \text{ mm}}{0.1 \text{ mm}} + 2(8 + 10) = 294 \quad (13)$$

$$nz = \frac{1.6 \text{ mm}}{0.4 \text{ mm}} + 2(8 + 10) = 40 \quad (14)$$

The following setup, as given in Table 3, was used to run the FDTD simulation on the MATLAB platform.

Table 3. FDTD Setup

Parameter	Value	Parameter	Value
nx	176	dx	0.1 mm
ny	294	dy	0.1 mm
nz	40	dz	0.4 mm
CPML buffer cells	8	Number of time steps	5000
Air buffer cells	10	Caurant factor	0.9

IV. RESULTS AND DISCUSSIONS

The proposed antenna was fabricated using an economical FR4 substrate and tested using Rohde & Schwarz Vector network analyzer (2 ports, 9 kHz - 13.6 GHz), model ZVL13. The prototype of the Giraffe-shaped antenna is shown in fig. 9. The overall dimensions of the substrate are 14 mm x 25.8 mm x 1.6 mm.

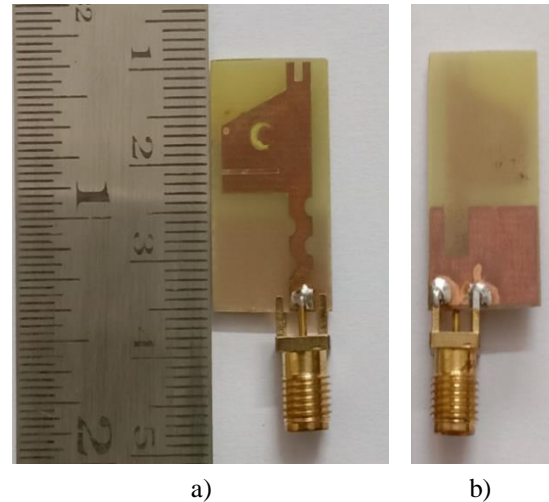


Fig. 9 Proposed fabricated antenna a) Top view b) ground plane

The S_{11} values obtained in the simulation are compared with measurement values. This comparison is shown in fig. 10. It is found that measured values of S_{11} are in good agreement with HFSS simulation and FDTD analysis. The -10 dB bandwidth obtained is from 3.2 GHz to 9.8 GHz. The bandwidth is 103.12% of the centre frequency 6.5 GHz.

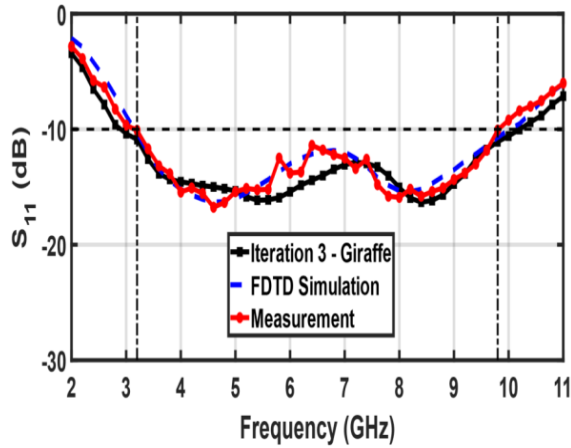


Fig. 10 Comparison of S_{11} – Iteration 3 - Giraffe Shaped antenna with FDTD analysis and Measurement results.

The proposed antenna's gain was measured and compared with simulated gain. The comparison is shown in fig. 11.

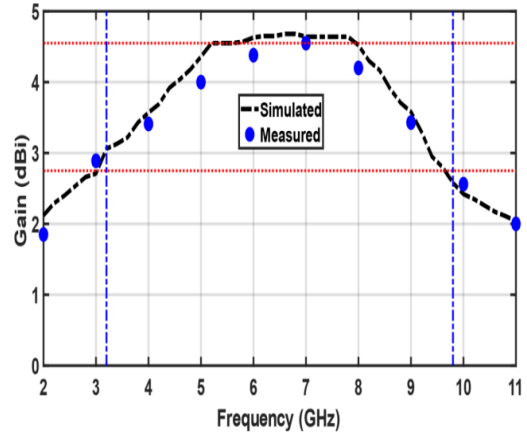


Fig. 11 Peak Gain – Simulated and Measured

The measured gain is close to the simulated gain over the entire bandwidth. The radiation patterns of the proposed antenna are measured at three frequencies 3.6 GHz, 6.6 GHz, and 9 GHz. The radiation patterns for co-planar and cross planar orientations are measured in the XZ and YZ planes. The radiation patterns are found stable over the impedance bandwidth. These simulated and measured radiation patterns at 3.6 GHz, 6.6 GHz, and 9.0 GHz are shown in fig. 12, 13, and 14, respectively. The measured patterns are analogous to simulated ones.

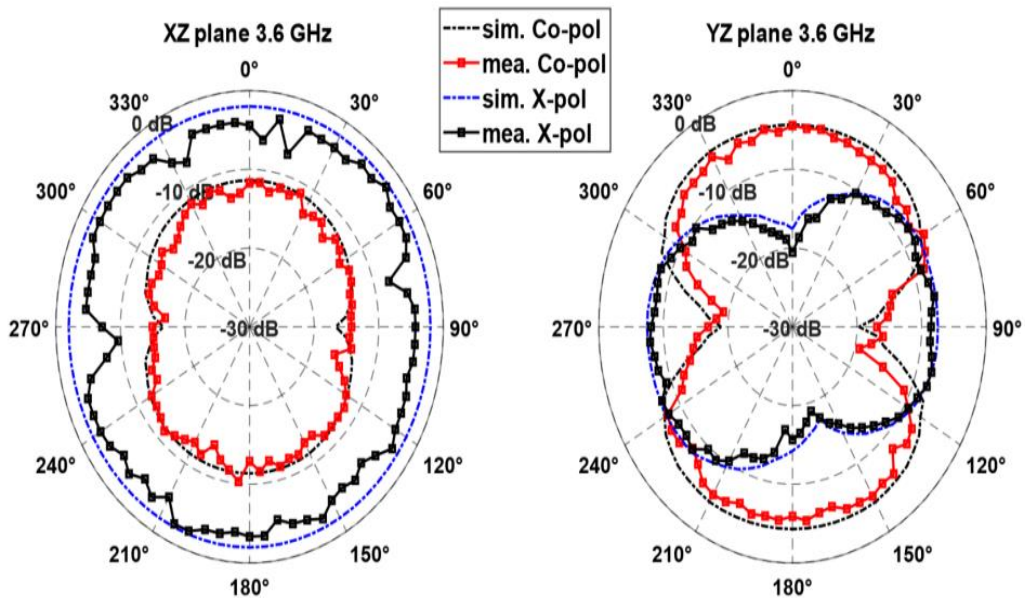


Fig. 12 Radiation patterns - Simulation and Measured 3.6 GHz

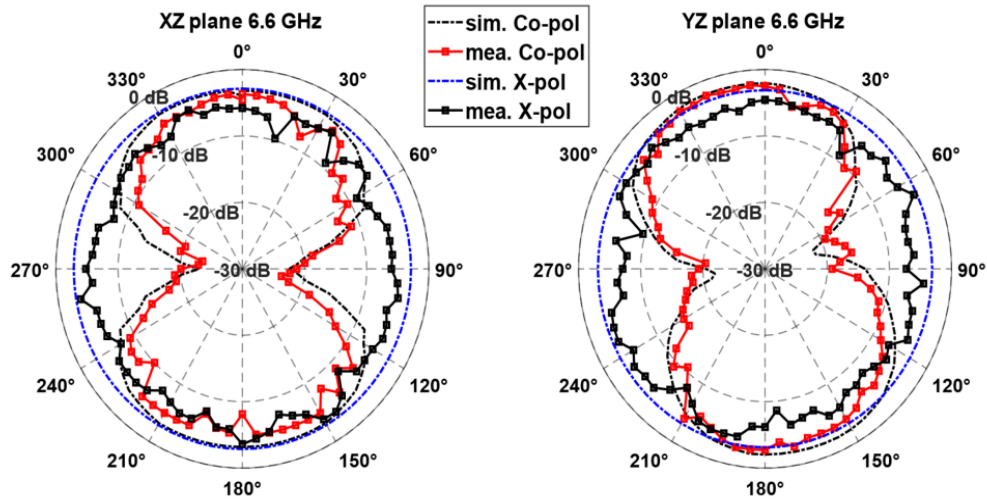


Fig. 13 Radiation patterns - Simulation and Measured at 6.6 GHz

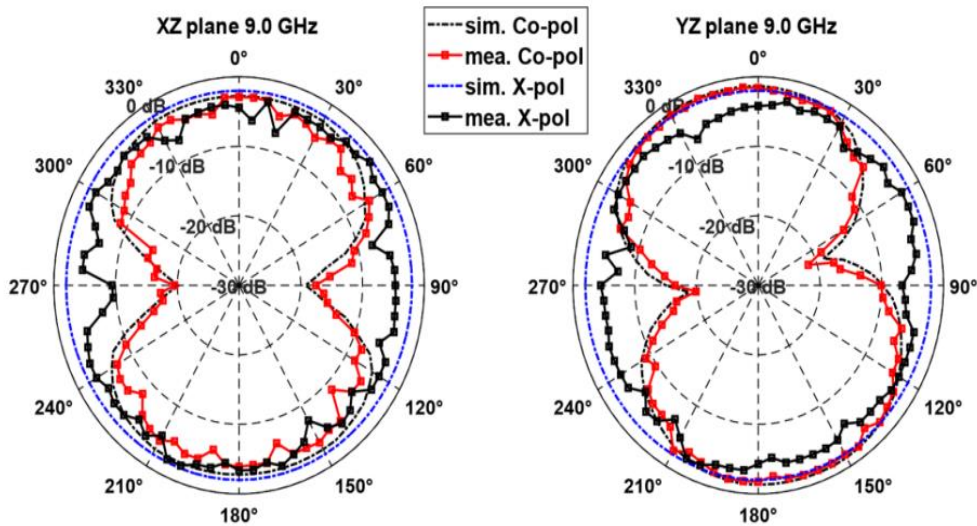


Fig. 14 Radiation patterns - Simulation and Measured at 9 GHz

Table 4. Comparison of proposed Giraffe shape antenna with other UWB antennas

Reference No.	Freq. Band (GHz)	Gain (dBi) Min - Max	Substrate and its height	Patch Area (mm ²)	Technique Used
5	3.0 – 10.0	2.0 – 7.5	FR4, 0.76 mm	45 x 50 (2250)	Elliptic shape with a central circular slot
6	4.6 – 9.0	0.55 – 1.3	F4B, 1.0 mm	36 mm Diameter (1017.87)	Three identical pairs of printed half-wave dipoles
7	3.05 – 11.9	2.1 - 5.2	FR4, 0.8 mm	23.7 x 23.7 (561.69)	Compact slot
10	3.1 - 10.6	3.33 – 5.66	FR4, 0.8 mm	24 x 24.4 (585.6)	Stepped triangular,
Proposed	3.2 – 9.8	2.74 – 4.45	FR4, 1.6 mm	14 x 25.8 (361.2)	Unwanted pixels removal

A qualitative comparative analysis of the proposed prototype is given in Table 4. The similarly reported prototypes to suffer from one or other reasons like the size of the antenna, its gain, and the complexity of the iteration process in the optimization process. In comparison with the above-cited references, the size of the proposed antenna is more compact. Further, the radiation patterns of the proposed antenna are more stable over the entire bandwidth. The gain of the proposed antenna is comparable with above all except [5]. However, in [5], the high gain of the order of 7.5 is observed for a small portion of the bandwidth, and for the rest of the bandwidth, it is similar to the proposed antenna. The implementation of HPSO in the proposed design is less complex than the one used in [10], considering the number of tiny dipoles used for the analysis. The validation of the simulation results with FDTD analysis is an added feature of the reported work in this paper. Hence, the proposed antenna is the best candidate for UWB applications.

V. CONCLUSION

A compact Giraffe-shaped antenna is designed using the HPSO algorithm. The antenna is fabricated using an FR4 substrate with overall dimensions of 14 mm x 25.8 mm x 1.6 mm. The proposed antenna offers an S_{11} less than -10 dB (more negative) over the bandwidth of 3.2 GHz to 9.8 GHz. The peak gain of the proposed antenna varies from 2.74 dBi to 4.45 dBi over the entire bandwidth. The performance of FDTD analysis using MATLAB code is encouraging for validation of non-regular shape antennas. The algorithm developed for implementing geometry is quite helpful for irregular shapes. The proposed antenna is a suitable choice for UWB applications.

In the future, the proposed method can be extended to design irregular-shaped antennas with different feed mechanisms and radiation patterns.

ACKNOWLEDGEMENT

The authors would like to acknowledge the co-operation extended by Dr Anand Kakade, Mr M.R. Jadhav, and Mr Vijay Patil of the Rajarambapu Institute of Technology, Sakharale Maharashtra, India, for the measurement of antenna parameters.

REFERENCES

- [1] P. S. Hall and Y. Hao, *Antennas and Propagation for Body-Centric Wireless Communications*, 2nd ed., Boston: Artech House, (2012).
- [2] J. Wei, X. Jiang, and L. Peng, "Ultrawideband and high-gain circularly polarized antenna with double-Y-shape slot," *IEEE Antennas Wireless Propagation Lett.* 16 (2017) 1508–1511, Jan. 2017.
- [3] N. Rahman, M. T. Islam, Z. Mahmud, and M. Samsuzzaman, "The broken-heart printed antenna for ultrawideband applications: design and characteristics analysis," *IEEE Antennas Propagation Mag.* 60(6) (2018) 45-51.
- [4] J. Wu, Z. Zhao, Z. Nie, and Q. Liu, "A printed UWB Vivaldi antenna using stepped connection structure between slotline and tapered patches," *IEEE Antennas Wireless Propagation Lett.* 13 (2014) pp 698-701.
- [5] N.C. Azenui, H.Y.D. Yang, "A printed crescent patch antenna for ultrawideband applications," *IEEE Antennas Wireless Propagation Lett.* 6 (2017) 113-116.
- [6] C. Yu, T. Xu, and C. Liu, "Design of a novel UWB omnidirectional antenna using particle swarm optimization," *International Journal of Antennas and Propagation*, 4 (2015) 1-7.
- [7] B. Gong, X.S. Ren, Y.Y. Zeng, L.H. Su, and Q.R. Zeng, "Compact slot antenna for ultra-wideband applications," *IET Microwaves Antennas and Propagation*, 8(3) (2014) 200-205.
- [8] S. K. Mishra, R.K. Gupta, A. Vaidya, and J. Mukherjee, "A compact dual-band fork-shaped monopole antenna for Bluetooth and UWB applications," *IEEE Antennas Wireless Propagation Lett.* 10 (2011) 627-630.
- [9] A. A. Deshmukh, P.V. Mohadikar, "Modified rectangular shape patch antennas for ultra-wideband and notch characteristics response," *Microwave Optical Technology Letters.* 59(7) (2017) pp 1524-1529.
- [10] M. A. Trimukhe, B.G. Hogade, "Design of the compact ultra-wideband (UWB) antenna bandwidth optimization using particle swarm optimization algorithm," *Iranian Journal of Electrical and Electronic Engineering.* 15(2) (2019) 195-202.
- [11] A. Bhattacharya, B. Roy, M. Islam, S.K. Chowdhury, and A.K. Bhattacharjee, "A UWB monopole antenna with hexagonal patch structure designed using particle swarm optimization algorithm for wireless applications," in *Proc. IEEE MicroCom'16.*, paper 11(3) (2016) 109-125.
- [12] Y. Li, W. Shao, L. You, and B. Wang, "An improved PSO algorithm and its application to UWB antenna design," *IEEE Antennas Wireless Propagation Lett.* 12 (2013) 1236-1239.
- [13] L. Wakrim, I. Saida, and M. M. Hasani, "The study of the ground plane effect on a multi-band PIFA antenna by using genetic algorithm and particle swarm optimization," *Journal of Microwave Optoelectronics and Electromagnetics Applications.* 15(4) (2016) 293–308, Oct.-Dec.2016
- [14] Rhea Nath, Promod Singh., "Designing and Analysis of MIMO Antenna for UWB Applications," *International Journal of Engineering Trends and Technology (IJETT)*, 56(1) (2018) 25-30.
- [15] A. Taflov and S. C. Hagness, *Computational Electrodynamics: The Finite-Difference Time-Domain Method*, Norwood MA: Artech House, (2000).
- [16] A. Elsherbeni and V. Demir, *The Finite-Difference Time-Domain Method for Electromagnetics with MATLAB Simulations*, 2nd ed., Raleigh, NC: SciTech, (2015).
- [17] A. Muscat J. A. Zammit, "A Microstrip Antenna Shape Grammar," chapter In Nasimuddin N, ed. *Microstrip Antennas.*, Rijeka, InTech., (2011) 251-272.
- [18] S. Sahoo, L.P. Mishra, and M. N. Mohanty, "Optimization of Z-shape microstrip antenna with I-slot using discrete particle swarm optimization (DPSO) algorithm," in *Proc. ICC-2016*, (2016) 91-98.
- [19] N. Feiz, F. Mohajeri, and D. Zari, "Design, simulation and fabrication of an optimized microstrip antenna with metamaterial superstrate using particle swarm optimization," *Progress in Electromagnetics Research M.*, 36 (2014) 101-108.
- [20] D. K. Naji, J. S. Aziz, and R. S. Fyath, "Design and simulation of miniaturized Minkowski fractal aperture-coupled antenna for 5.8 GHz RFID applications," *Journal of Emerging Trends in Computing and Information Sciences.* 3(7) (2012) 1013-1020.
- [21] W. Weng, C.T.M. Choi, and S. Wang, "Optimal feed positions for micro stripline-fed rectangular patch antennas by finite difference time domain analysis," in *Proc. Asia-Pacific Microwave Conference 2001*(2001) 1342-1345.
- [22] ZH. Qian, Ru-S. Chen, K. Leung, and H. Yang, "FDTD analysis of microstrip patch antenna covered by plasma sheath," *Progress In Electromagnetics Research, PIER.* 52 (2005) 173-183.
- [23] E. Nishimaya, M. Aikawa, "FDTD analysis of stacked microstrip antenna with high gain," *Progress In Electromagnetics Research, PIER.* 33 (2001) 29-43.
- [24] Y. El. Hajibi, A. El. Hamichi, "Simulation and numerical modelling of a rectangular patch antenna using finite difference time domain (FDTD) method," *Journal of Computer Science and Information Technology.* 2(2) (2014) 01-08.
- [25] A. Boufrioua, E. Ksouri, and M. Harbadji, "Study by the FDTD Method of Multiband Microstrip Patch Antenna Loaded with L-Shaped Slot," in *Proc. IEEE/ACS 16th International Conference on Computer Systems and Applications (AICCSA)*, (2019) 1-4.
- [26] G. G. Bhide, A. B. Nandgaonkar, and S. L. Nalbalwar, "On the novel image algorithms filling material index over the finite-difference time-domain grid for analysis of microstrip patch antenna using MATLAB," in *Proc. Iyer B, Rajurkar A, Gudivada V, eds. Applied Computer Vision and Image Processing. Advances in Intelligent Systems and Computing*, (1155), Singapore: Springer, (2020) 139-149.